Received: 20 March 2017 | Accepted: 18 July 2017

DOI: 10.1002/hyp.11283

WILEY

RESEARCH ARTICLE

The role of eddies in solute transport and recovery in rock fractures: Implication for groundwater remediation

Seung Hyun Lee[1] | In Wook Yeo[2] | Kang-Kun Lee[3] | Won Sang Lee[1]

[1] Unit of Ice Sheet and Sea Level Changes, Korea Polar Research Institute, 26 Songdomirae-ro, Yeonsu-gu, Incheon 21990, Republic of Korea

[2] Department of Geological and Environmental Sciences, Chonnam National University, 77 Yongbong-ro, Buk-gu, Gwangju 61186, Republic of Korea

[3] School of Earth and Environmental Sciences, Seoul National University, 1 Gwanak-ro, Gwanak-gu, Seoul 08826, Republic of Korea

Correspondence
In Wook Yeo, Department of Geological and Environmental Sciences, Chonnam National University, 77 Yongbong-ro, Buk-gu, Gwangju 61186, Republic of Korea.
Email: iwyeo@chonnam.ac.kr

Funding information
Basic Science Research Program; Ministry of Education, Grant/Award Number: 2015R1D1A1A01057718; Ministry of Oceans and Fisheries, Grant/Award Number: PM17020; Korea Ministry of Environment, Grant/Award Number: 2015000550002

Abstract

A better understanding of solute transport and retention mechanism in rock fractures has been challenging due to difficulty in their direct observations in microscale rough-walled fractures. Six representative troughs in a rough-walled fracture were selected for microscale observations of eddy formation with increasing flow velocity and its effect on spatiotemporal changes of solute concentration. This experimental study was enabled by a microscale visualization technique of micro particle image velocimetry. With increasing flow velocity (Re ≤ 2.86), no eddies were generated, and solutes along the main streamlines transported rapidly, whereas those near the wall moved slowly. A larger amount of solutes remained trapped at all troughs at Re = 2.86 than Re < 1. For Re = 8.57, weak eddies started to be developed at the troughs on the lee side, which little contributed to overall solute flushing in the fracture. Accordingly, a large of amount of water was needed for solute flushing. The flow condition of 1 < Re < 10, before a full development of eddies, was least favourable in terms of time and amount of remediation fluid required to reach a target concentration. After large eddies were fully developed at troughs on the lee side for Re = 17.13, solutes were substantially reduced by eddies with less amount of water. Fully developed eddies were found to enhance solute transport and recovery, as opposed to a general consensus that eddies trap and delay solutes. Direct inflow into troughs on the stoss side also made a great contribution to solute flushing out of the troughs. This study indicates that fully developed eddies or strong inflows at troughs are highly possible to form for Re > 10 and this flow range could be favourable for efficient remediation.

KEYWORDS

eddies, immobile fluid zone, recovery, rock fracture, solute transport, visualization technique

1 | INTRODUCTION

A fundamental understanding of solute transport mechanisms in fractured rocks is requisite for accurate estimation of travel and residence time of solutes for solute transport and groundwater remediation. The advection–dispersion equation has been used to model the fate and transport of solute or contaminant in groundwater (Zheng & Bennett, 2002):

$$\frac{\partial C}{\partial t} = \frac{\partial}{\partial x_i}\left(D_{ij}\frac{\partial C}{\partial x_j}\right) - \frac{\partial}{\partial x_i}(v_i C), \quad (1)$$

where C is the solute concentration, t is the time, D_{ij} is the dispersion tensor, and v_i is the groundwater velocity. In Equation 1, the dispersion assumes the Fickian behaviour, where the spatial distribution of the solutes becomes Gaussian for a slug of solute (Bodin, Delay, & de Marsily, 2003; Dagan, 1989).

However, numerical studies and laboratory and field tracer tests, conducted for rock fractures, have reported non-Fickian behaviour, characterized as early arrivals and long tails in the breakthrough curve (Becker & Shapiro, 2000; Boutt, Grasselli, Fredrich, Cook, & Williams, 2006; Cardenas, Slottke, Ketcham, & Sharp, 2007; Raven, Novakowski, & Lapcevic, 1988; Qian, Chen, Zhan, & Luo, 2011). As shown in Figure 1, non-Fickian dispersion has been attributed to many origins such as sorption (Neretnieks, Eriksen, & Tähtinen, 1982), channelling, or tortuous flow (Moreno, Neretnieks, & Eriksen, 1985; Tsang & Tsang, 1987), fracture heterogeneity (Bauget & Fourar, 2008; Wang & Cardenas, 2014), diffusive mass transfer with rock matrix (Lapcevic, Novakowski, & Sudicky, 1999; Novakowski, Lapcevic, Voralek, & Bickerton, 1995; Zhou, Liu, Bodvarsson, & Molz, 2006), and trapping

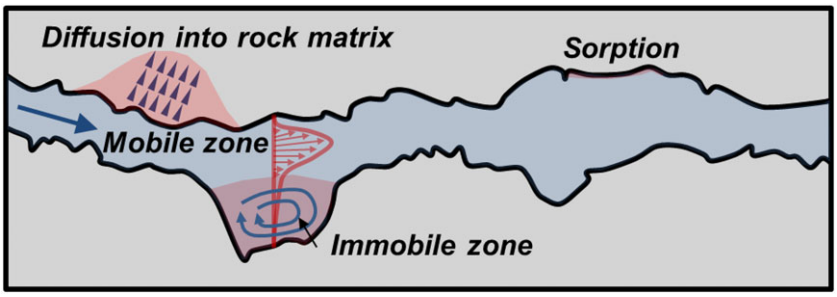

FIGURE 1 Conceptual diagram showing main causes of non-Fickian transport in a rough-walled fracture

of solutes in immobile fluid zones (Boutt et al., 2006; Cardenas et al., 2007; Bolster, Méheust, Le Borgne, Bouquain, & Davy, 2014).

Unlike the other causes of non-Fickian dispersion, the mass transfer processes between mobile and immobile fluid zones are speculative and conceptual, mainly due to difficulty in directly observing the phenomena of flow and solute transport actually occurring within microscale rough-walled fractures. However, the recent development of numerical techniques enough to solve the Navier–Stokes equations has led to many numerical investigations of the role of eddies in solute transport (Bolster et al., 2014; Bouquain, Méheust, Bolster, & Davy, 2012; Boutt et al., 2006; Cardenas et al., 2007; Cardenas, Slottke, Ketcham, & Sharp, 2009; Qian et al., 2011). These numerical studies presented that eddies accounted for non-Fickian behaviour and exerted an important influence on solute transport and retention.

Eddy (or recirculation zone) acts as immobile zone and occurs due to the irregularities of apertures in a rough-walled fracture (Cardenas et al., 2009; Raven et al., 1988). Mass exchange between mobile and immobile zones is assumed to be diffusive, which is based on the mobile–immobile conceptual models and their relevant analytical equations that have been suggested to explain non-Fickian process (Cherubini, Giasi, & Pastore, 2013; Gao, Zhan, Feng, Fu, & Huang, 2012; Hansen, Berkowitz, Vesselinov, O'Malley, & Karra, 2016; Qian et al., 2011; Raven et al., 1988). Cardenas et al. (2009) showed that tailing, due to a large eddy, was more persistent with an increase of the Reynolds number (Re) up to about 10. Eddies were shown to be distinctly separated from main flow channel, where only a possible mass transfer process is diffusion between mobile fluid zones and eddies.

Further, the phenomena of tailing and rebound are commonly observed during pump-and-treat, which presents the major barrier to achieving remediation goals (USEPA, 1996; Voudrias, 2001). One of physical and chemical processes, causing a rebound in contaminant concentration associated with the pump-and-treat, is mass exchange between immobile and mobile zones (Cohen, Vincent, Mercer, Faust, & Spalding, 1994; Harvey, Haggerty, & Gorelick, 1994; Luo et al., 2005; Luo et al., 2006; de Barros, Fernàndez-Garcia, Bolster, & Sanchez-Vila, 2013). Therefore, it is natural that solutes trapped within eddies in troughs of fracture walls impede their transport and remediation.

However, the assumption of the so-called "isolated" eddies and diffusive mass exchange between mobile fluid zones and eddies was recently questioned. Lee, Yeo, Lee, and Detwiler (2015) first observed, from microscale rough-walled fracture, that eddies were no longer isolated and instead were connected to the mobile flow zones by advective paths, as opposed to the above-mentioned 2D fracture geometry-based numerical studies. Lee et al. (2015) explained that these opposing results originated from fracture geometries. This advective paths connecting eddies to the main flow channel take place at three-dimensional (3D) nature of real fractures where surface roughness leads to variations in fracture aperture in all directions so that large aperture regions tend to be isolated. Richmond, Perkins, Scheibe, Lambert, and Wood (2013) also showed through numerical studies that the velocity transient fluctuation in an idealized sinusoidal-walled tube channel at Re of 449 decreased the amount of tailing in eddies, consequently reducing the rate of increase of longitudinal dispersion with Re.

In these respects, more direct observation-based thorough studies are demanded for a fundamental understanding of the role of eddies in solute transport and groundwater remediation in a rough-walled fracture. This study is a follow-up study of our previous work (i.e., Lee et al., 2015) with emphasis on the implication for groundwater remediation. The originality of this study lies in direct microscale observation of formation and evolution of eddies and spatiotemporal changes of solute concentrations at troughs in a rough-walled fracture. With a microscale visualization technique of micro particle image velocimetry (micro-PIV), we investigate how eddies are developed with flow velocity and play a role in solute transport. Eddies can occur at the larger aperture areas even for Re < 1 (Boutt et al., 2006; Cardenas et al., 2007) and, in general, grow as inertial forces increase (Re > 1), as such in single-well push–pull tracer tests and groundwater remediation works carried out under high velocity flow. Therefore, we observe flow structure and solute movement at six local troughs on fracture wall, where eddies are highly possible to occur, for a full range of Re = 0.08 to 17.13 to cover viscous and inertial forces-dominant flows. This study also provides a discussion regarding an efficient extraction of contaminants trapped in rough-walled fractures by utilizing eddies.

2 | EXPERIMENTAL METHODS

2.1 | Fracture preparation

A rough-walled fracture, 200 mm long by 1 mm wide, was prepared by scanning both surfaces of a rough-walled fracture and engraving them on acrylic. The scanned surfaces were repeated approximately 6 times to make a 200-mm-long flow channel (Figure 2a). Apertures varied from 387 to 2,487 μm with an arithmetic mean aperture and a standard deviation of 1,030 and 411 μm, respectively (refer to Lee, Lee, & Yeo, 2014 for more detailed information on the fracture geometry).

Considering the results that eddies are generated at the larger aperture area (Cardenas et al., 2007) and in the lee side of fracture

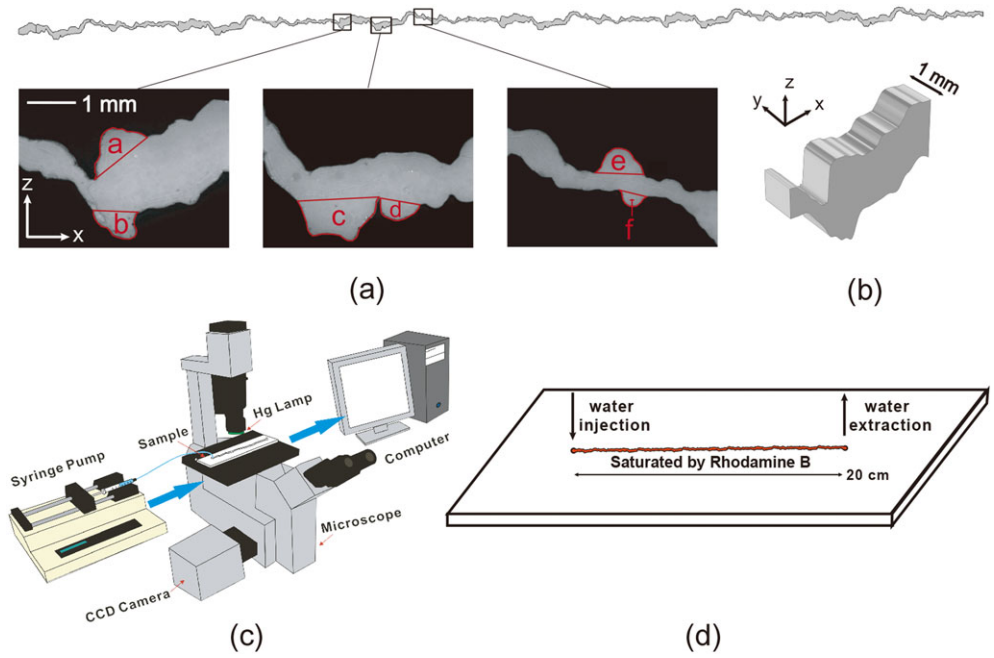

FIGURE 2 Fracture geometry and experimental set-up. (a) Six representative troughs (Subregions a to f) selected for microscale observation of flow and solute transport, (b) 3-D fracture geometry of Subregions a and b of the fracture, (c) a microscale visualization technique of micro particle image velocimetry (micro-PIV) system, and (d) set-up for solute transport and recovery experiments

walls (Boutt et al., 2006), representative six local subregions, as shown in Figure 2a, were selected to monitor the formation and evolution of eddies and subsequent solute transport at troughs of fracture wall. Subregions a to d represented the largest aperture area, where Subregions a and d were troughs mostly on the lee side and Subregions b and c were troughs possibly on the stoss side that received direct inflow. Subregions e and f were chosen to represent the troughs at the smallest aperture area for comparison purpose.

Apertures changed only in the *x* axis and did not change in the *y* axis (Figure 2b). The front and rear lateral boundaries (the faces normal to the *y* axis) were no-flow ones. This fracture geometry differed from the 2D fracture where the fracture was implicitly assumed to be infinite in the *y* direction. Lee et al. (2015) proved that this kind of fracture geometry showed a clear 3D trajectory of streamlines occurring in the isolated large aperture.

2.2 | Experimental set-up

Micro-PIV system consisted of an inverted microscope (Olympus IX-50), syringe pump, charge-coupled device (CCD) camera, mercury lamp, and computer (Figure 2c). Flow structures were important for better interpretation of solute transport. Therefore, we first carried out flow experiments to observe the development of flow paths and eddies at each subregion for the same representative flow condition as in the solute transport and recovery experiments (explained below). Deionized water mixed with 1-μm-diameter fluorescent particles was injected into the left inlet of the fracture at constant flux ranging from 0.3 to 60 ml/hr, which corresponded to Re = 0.08 to 17.13 ($Re = \rho Ub/\mu$, where U is the macroscopic fluid velocity, calculated by injection flow rate divided by fracture cross-sectional area, i.e., arithmetic mean aperture times fracture width, b is the arithmetic mean aperture, ρ is the water density, and μ is the water viscosity). For each flow conditions, images acquired at subregions yielded flow paths (streamlines) traced out by fluorescent particles moving with the flow.

For solute transport and recovery experiments, Rhodamine B (fluorescent dye) was diluted with deionized water to achieve a maximum dynamic range (i.e., peak concentration occurred near the sensitivity limit of the light/camera system). First, we saturated the fracture with diluted Rhodamine B (Figure 2d). The three snapshots of Figure 2a that were brightened by Rhodamine B represented the initial state at each subregion. Then, deionized water with no fluorescence was injected into the left inlet of the fracture to form flow conditions of Re = 0.08, 0.29, 2.86, 8.57, and 17.13. The corresponding Peclet numbers ($Pe = Ub/D_m$) were 238, 795, 7,948, 23,843, and 47,658, respectively, where molecular diffusion coefficient (D_m) of Rhodamine B is 3.6×10^{-10} m^2/s.

Although the fracture saturated with diluted Rhodamine B was being flushed with deionized water, the snapshots in every subregion were continuously captured by CCD camera (Figure 3) until the fluorescence intensity in the fracture became dim. Each captured image had 344 pixels in horizontal direction and 260 pixels in vertical direction. Pixel size was 12.6 μm. The captured images were used to calculate solute concentration at each subregion. Fluorescence intensity (or brightness) is linearly proportional to dye concentration in dilute samples (Lakowicz, 2006). At the initial state before starting the flushing with deionized water (i.e., the upper figure of Figure 3b), fluorescence intensities of pixels falling in each subregion were summed, and this total intensity value represented initial solute concentration (C_0). Brightness of the captured images became dim with increasing the volume of injected deionized water. The same procedure applied to these images to calculate solute concentration C_{PV}, where C_{PV} was concentration at corresponding pore volume (PV) and one PV was calculated by arithmetic mean aperture times fracture width times fracture length. The conversion of intensity to concentration proved valid in

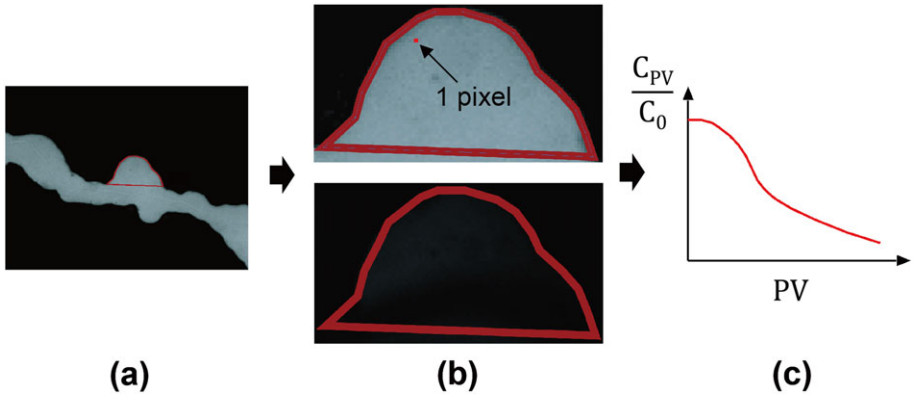

FIGURE 3 (a) Snapshot image showing initial condition (C_0) of the fracture saturated with Rhodamine B, (b) upper image showing one pixel size (12.6 μm) of the image captured by CCD camera and bottom one showing a state of a full removal of Rhodamine B from the fracture by injecting deionized water, and (c) an example of relative concentrations (C_{PV}/C_0) plot with injected pore volume (PV)

our previous study (Lee et al., 2015). As shown in Figure 3c, relative concentration (C_{PV}/C_0) at each subregion was plotted against the injected PV.

3 | RESULTS AND DISCUSSIONS

3.1 | Flow structures

For flow experiments carried out at the flow condition of Re = 0.08, 0.29, 2.86, 8.57, and 17.13, images were acquired at subregions with micro-PIV, which demonstrated how flow structure changed with increasing flow velocity (Figure 4). For low flow condition of Re < 1, dots of fluorescent particles were clearly identified, and no eddies were developed at all subregions. When particles, passing through the observed frames of micro-PIV, moved faster than the shutter speed of CCD camera installed on micro-PIV, they were observed as streamlines rather than dots. From Re = 0.29, main streamlines started to be observed around the middle plane of the fracture, whereas fluorescent particles were observed as dots near the fracture wall. This indicated an increase of the contrast in flow velocity between the middle plane and the fracture wall.

For flow condition of Re = 2.86, main streamlines were well developed around the middle plane of the fracture. Dots of fluorescent

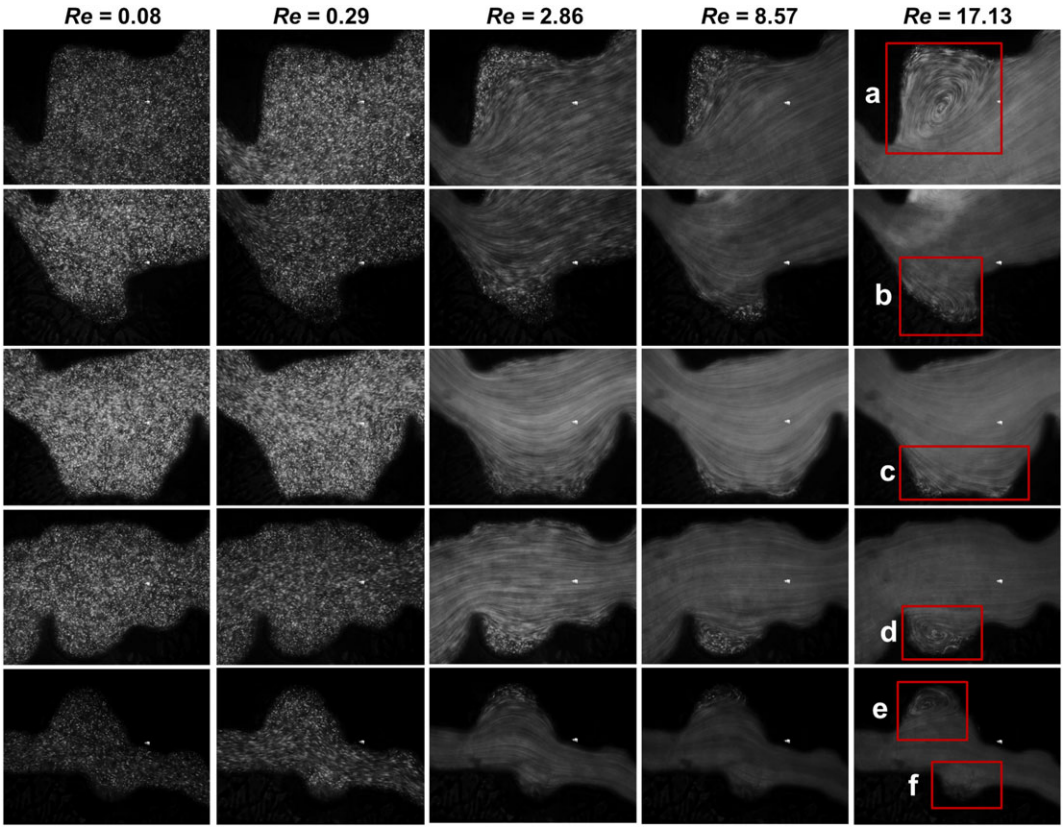

FIGURE 4 Microscopic observation of flow structures, including the evolution of eddies, at six subregions with increasing flow velocity from 0.08 to 17.13

particles were clearly identified at each subregion, indicating that flow velocity was very small at the troughs of fracture wall, compared to that in the main streamlines. Clear development of eddies was not observed at any subregions.

For Re = 8.57, clear eddies were observed at Subregions d and e. At Subregion a, even though eddies were not seen in Figure 4, continuous captured images showed that particles moved backward and swirled around within the trough, indicating very weak eddies. When the overall flow velocity increased to Re = 17.13, eddies were fully developed at the Subregions a, d, and e. Because of a strong inward flow into Subregions b and c, only slight eddies were observed, and a full formation of recirculation zone was restricted. Despite poor brightness and resolution, the full formation of eddies was supposed not to occur at Subregion f. In conclusions, a full development of eddies, showing a full recirculation zone, was found on the lee side.

3.2 | Effect of eddies on solute transport and recovery

Figure 5 shows the spatial distribution of solutes at all subregions for flow conditions of Re = 0.08, 0.29, 2.86, 8.57, and 17.13. The snapshots taken at PV = 0 represented the initial state (C_0) at each subregion. When deionized water with no fluorescence was injected into the left inlet of the fracture, the solutes were flushed out.

For Re ≤ 0.29, solutes along the main streamlines were first flushed out, and those near the wall then disappeared. The overall pattern was that solute concentration gradually decreased from the main streamlines to the wall, which confirmed that flow velocity was higher near the central streamline and lower near the fracture wall.

For Re = 2.86, no eddies were still generated. Solutes along the central streamline disappeared more rapidly, whereas those near the wall were flushed out more slowly than for Re = 0.29. This is due to the greater vertical velocity contrast across the aperture with increasing Re. A large amount of solutes remained trapped at all subregions even after PV = 0.70, which was clearly distinguished from Re = 0.29. This indicates that solute transport and remediation can be highly delayed by the troughs of rough-walled fractures, which results in the heavy tails.

For Re = 8.57, solute concentration became lower at Subregions b, c, and f than that of Re < 8.57. The inward flow into the subregions led to a decrease in solute concentration. Weak eddies, developed at Subregions a, d, and e, little contributed to reducing solute concentration.

When the flow increased to Re = 17.13, eddies were fully developed at Subregions a and d on the lee side of fracture wall. The solute concentrations at most of the subregions (troughs) were much lower than those at Re = 2.86 and 8.57. This strongly indicated that solutes trapped in the troughs, especially on the lee side, were flushed out by eddies and the strong inward flow also helped solute flushing at Subregions b and c (see PV = 0.45 and 0.70 in Figure 5). Fully developed eddies in troughs were found to enhance solute transport and recovery.

For Re = 8.57 and 17.13, the flushing patterns were clearly different from those of Re ≤ 2.86. For Re ≤ 2.86, as solutes moved out, the middle of the fracture was first dim and the regions near fracture walls became sequentially dim at later times. However, the high concentration band in the middle of the fracture was observed for Re ≥ 8.57 with solutes being flushed out. This is because the solutes were flushed out of the troughs and cast into the middle of the fracture by either eddies or direct inflows, and the solutes then travelled along the main streamlines at later times. This observation was in good agreement with Lee et al. (2015). They showed that the fully grown eddies formed advective paths between the main flow channel and the recirculation zone.

3.3 | Implications for groundwater remediation

Trapping of solutes or contaminants in the troughs of the fracture wall impedes an efficient extraction of contaminants in rough-walled fractures. Solute behaviour in a trough with increasing flow velocity gives a valuable insight into groundwater remediation in rough-walled fractures, for which the relative concentrations (C_{PV}/C_0) with injected PV were plotted for Re = 0.08 to 17.13 (Figure 6). Solute concentration dropped at all subregions with the least PV for Re = 0.08. With increasing Re up to 2.86, the required PV increased to reach the same relative concentration. In particular, the required PV increased significantly from Re = 0.29 to 2.86. This was due to solute trapping at the troughs

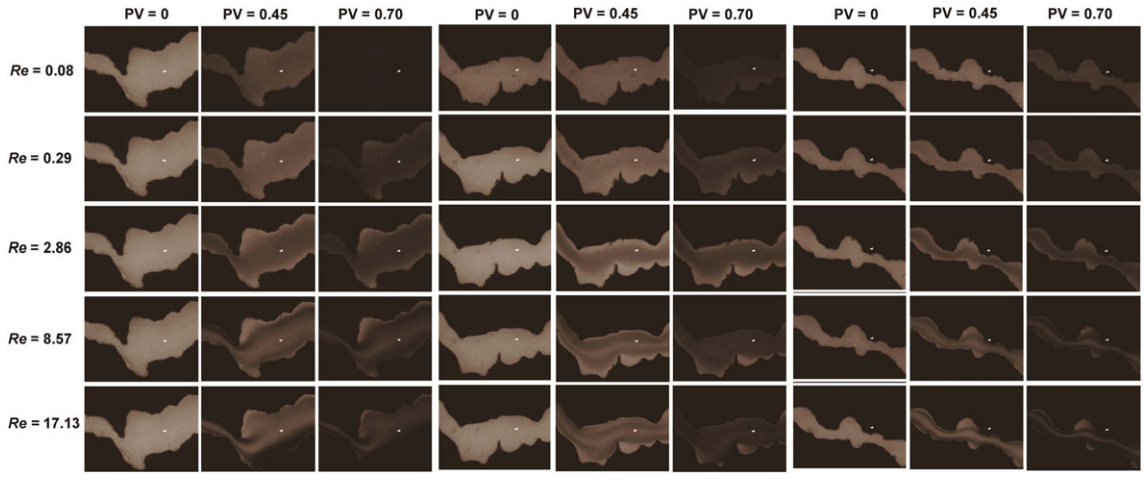

FIGURE 5 Observed images of spatial distribution of solutes (diluted Rhodamine B) being flushed out at each subregion for Re = 0.08, 0.29, 2.86, 8.57, and 17.13

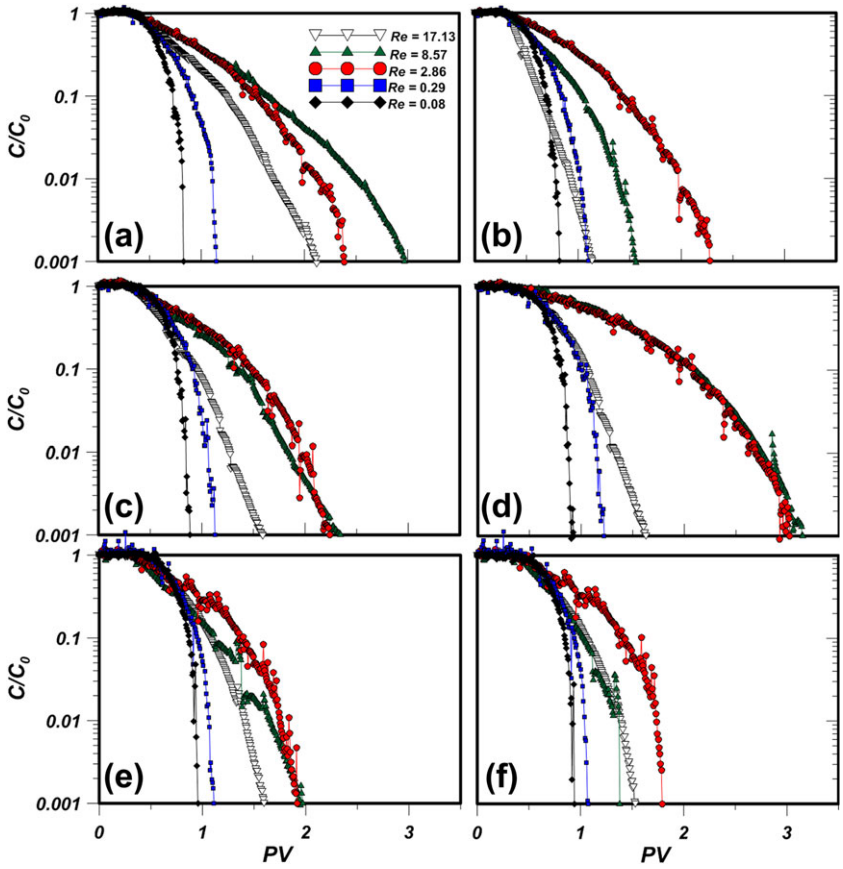

FIGURE 6 Plots of relative concentration changes with pore volume (PV) at Subregions a to f

and the increased contrast in flow velocity between the main streamlines and the wall, as observed in Figure 4. This was also supported by higher concentrations at the troughs (subregions) and near the fracture wall for Re = 2.87 than those for Re = 0.29 (Figure 5).

For Re = 8.57, the relative concentration curves were clearly reversed at Subregions b, c, and f; that is, the required PV decreased with increasing Re from 2.86 to 8.57. This is because the inward flow into the subregions swept solutes away. At Subregion a on the deep lee side, very weak eddies were observed, but the required PV increased. Subregion d on the lee side and Subregion e had weak eddies, which little contributed to solute flushing.

After eddies were fully developed at Subregions a, d, and e for Re = 17.13, the amount of injected PV was substantially reduced. The required PV was also substantially reduced at Subregions b and c, mainly owing to strong inward flow. For all subregions, the required PV was significantly reduced. This provides important implication that solutes often trapped in the troughs, regardless of the stoss or the lee sides, can be flushed out by either strong inward flow or eddies.

Figure 7a showed the required amount ($PV_{0.001C_0}$) of PV to reach $0.001C_0$. For all subregions, the required $PV_{0.001C_0}$ increased for Re ≤ 2.86. As discussed above, solute trapping at the troughs and the increased velocity contrast between the main streamlines and the wall increased solute dispersion over the fracture. The peak $PV_{0.001C_0}$ was reached at Re = 2.86 for Subregions b and f, and Re = 8.57 for Subregions a and d on the less side.

For Re = 17.13, where large eddies were developed at Subregions a and d, $PV_{0.001C_0}$ was significantly reduced. Eddies developed at Subregion e also reduced $PV_{0.001C_0}$. $PV_{0.001C_0}$ was also decreased at Subregions b and c due to strong inward flows. This indicates that the overall remediation efficiency over the fracture can be clearly improved after eddies are fully developed, as opposed to a general consensus that solutes trapped at the troughs in rough-walled fractures impede their

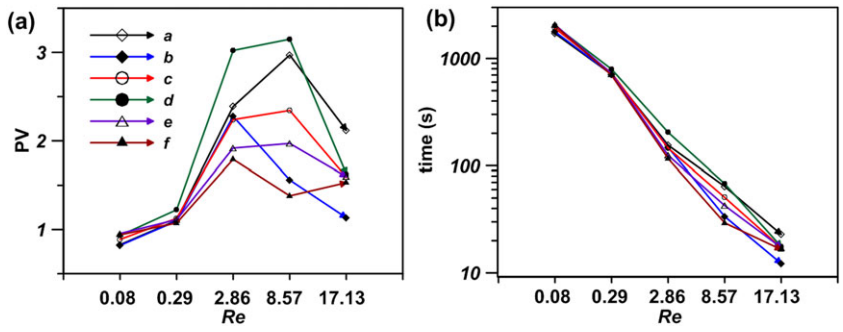

FIGURE 7 (a) Required pore volume (PV) and (b) time for reducing residual concentration to $0.001C_0$ for Re = 0.08, 0.29, 2.86, 8.57, and 17.13

recovery and consequently require a large volume of water for groundwater remediation.

The average amount of $PV_{0.001C_0}$ for all selected subregions was calculated as 0.89, 1.12, 2.27, 2.23, 1.60 at Re = 0.08, 0.29, 2.86, 8.57, and 17.13, respectively. The least $PV_{0.001C_0}$ was achieved at the lowest flow condition of Re = 0.08, which did not mean efficient recovery or groundwater remediation. Figure 7b showed the required time to reach $0.001C_0$. It is natural that an increase in flow velocity reduces the required time. For Re < 1, solutes were flushed out with relatively small amount of water, but as we expected, low flow velocity can be inefficient for remediation due to a large required time. Before a full development of eddies, the remediation of solutes trapped at the troughs could be least efficient, considering both time and amount of water. High flow velocity of Re = 17.13 resulted in fully developed eddies or direct inflow at the troughs, making remediation efficiency improved in terms of time and amount of remediation fluid.

4 | CONCLUSIONS

With new visualization technique of micro-PIV, we made microscale observations of eddy formation with increasing flow velocity and its effect on temporal changes of solute concentration at the troughs of fracture wall. For low flow velocity condition of Re < 2.86, clear development of eddies was not observed at all troughs. Main streamlines were well observed near the middle plane of the fracture, and the flow contrast between the middle plane and the wall increased with overall flow velocity. With increasing Re from 0.08 to 2.86, solutes along the main streamlines moves rapidly, whereas those near the walls were flushed out more slowly. A larger amount of solutes remained trapped at all troughs at Re = 2.86. This indicates that solutes can be highly delayed by troughs, which results in heavy tails.

For Re = 8.57, weak eddies started to be developed at Subregions a, d, and e, which little contributed to overall solute flushing in the fracture. A large volume of water for solute flushing was still required. Eddies were fully developed at troughs on the lee side for Re = 17.13. A fully developed eddies substantially reduced solutes trapped at the troughs with less amount of water and less time. For Re ≥ 8.57, direct inflow into the troughs on the stoss side led to efficient solute flushing. This is opposed to a general consensus that solutes are trapped at the troughs in rough-walled fractures, which impedes their recovery and consequently requires more volume of water for efficient remediation. Full eddies make remediation efficiency improved in terms of both time and amount of water.

This study indicates that for Re > 10, fully developed eddies and strong inward flow are highly possible to form at the troughs on either the lee side or the stoss side, respectively, which enhanced solute transport and recovery and was of help to efficient remediation. The flow condition of 1 < Re < 10 can be unfavourable in terms of time and amount of remediation fluid required to reach a target concentration, and that of Re < 1 can be also inefficient considering time. Groundwater pumping renders hydraulic gradient (i.e., Re) greater in the well vicinity and smaller with increasing radial distance. Therefore, the optimization of a number of the wells and their distances is requisite for efficient remediation utilizing fully developed eddies.

ACKNOWLEDGMENTS

This research was supported by Basic Science Research Program through the National Research Foundation of Korea (NRF) funded by the Ministry of Education (2015R1D1A1A01057718), Korea Polar Research Institute (KOPRI) project (Grant PM17020) funded by the Ministry of Oceans and Fisheries, and the Korea Ministry of Environment as "The GAIA Project (2015000550002)."

ORCID

In Wook Yeo http://orcid.org/0000-0002-0570-2023

REFERENCES

Bauget, F., & Fourar, M. (2008). Non-Fickian dispersion in a single fracture. *Journal of Contaminant Hydrology*, *100*, 137–148.

Becker, M. W., & Shapiro, A. M. (2000). Tracer transport in fractured crystalline rock: Evidence of nondiffusive breakthrough tailing. *Water Resources Research*, *36*, 1677–1686.

Bodin, J., Delay, F., & de Marsily, G. (2003). Solute transport in a single fracture with negligible matrix permeability: 1. Fundamental mechanisms. *Hydrogeology Journal*, *11*, 418–433.

Bolster, D., Méheust, Y., Le Borgne, T., Bouquain, J., & Davy, P. (2014). Modeling preasymptotic transport in flow with significant inertial and trapping effects—The importance of velocity correlations and a spatial Markov model. *Advances in Water Resources*, *70*, 89–103.

Bouquain, J., Méheust, Y., Bolster, D., & Davy, P. (2012). The impact of inertial effects on solute dispersion in a channel with periodically varying aperture. *Physics of Fluids*, *24*. 083602

Boutt, D. F., Grasselli, G., Fredrich, J. T., Cook, B. K., & Williams, J. R. (2006). Trapping zones: The effect of fracture roughness on the directional anisotropy of fluid flow and colloid transport in a single fracture. *Geophysical Research Letters*, *33*. L21402

Cardenas, M. B., Slottke, D. T., Ketcham, R. A., & Sharp, J. M. Jr. (2007). Navier-Stokes flow and transport simulations using real fractures shows heavy tailing due to eddies. *Geophysical Research Letters*., *34*(14). L14404

Cardenas, M. B., Slottke, D. T., Ketcham, R. A., & Sharp, J. M. Jr. (2009). Effects of inertia and directionality on flow and transport in a rough asymmetric fracture. *Journal of Geophysical Research*, *114*. B06204

Cherubini, C., Giasi, C. I., & Pastore, N. (2013). Evidence of non-Darcy flow and non-Fickian transport in fractured media at laboratory scale. *Hydrology and Earth System Sciences*, *17*, 2599–2611.

Cohen, R., Vincent, A., Mercer, J., Faust, C., & Spalding, C. (1994). Methods for monitoring pump-and-treat performance, EPA/600/R-94/123, R.S. Kerr Environ. Res. Lab., Ada, Okla., USA.

Dagan, G. (1989). *Flow and transport in porous formation*. New York, NY: Springer.

de Barros, F. P. J., Fernàndez-Garcia, D., Bolster, D., & Sanchez-Vila, X. (2013). A risk-based probabilistic framework to estimate the endpoint of remediation: Concentration rebound by rate-limited mass transfer. *Water Resources Research*, *49*(4), 1929–1942.

Gao, G., Zhan, H., Feng, S., Fu, B., & Huang, G. (2012). A mobile-immobile model with an asymptotic scale-dependent dispersion function. *Journal of Hydrology*, *424-425*, 172–183.

Hansen, S., Berkowitz, B., Vesselinov, V. V., O'Malley, D., & Karra, S. (2016). Push-pull tracer tests: Their information content and use for characterizing non-Fickian, mobile-immobile behavior. *Water Resources Research*, *52*, 9565–9585.

Harvey, C., Haggerty, R., & Gorelick, S. (1994). Aquifer remediation: A method for estimating mass transfer rate coefficients and an evaluation of pulsed pumping. *Water Resources Research*, *30*(7), 1979–1991.

Lakowicz, J. R. (2006). *Principles of fluoresence spectroscopy*. New York, NY: Springer.

Lapcevic, P. A., Novakowski, K. S., & Sudicky, E. A. (1999). The interpretation of a tracer experiment conducted in a single fracture under conditions of natural groundwater flow. *Water Resources Research*, *35*, 2301–2312.

Lee, S. H., Lee, K. K., & Yeo, I. W. (2014). Assessment of the validity of Stokes and Reynolds equations for fluid flow through a rough-walled fracture with flow imaging. *Geophysical Research Letters*, *41*(13), 4578–4585.

Lee, S. H., Yeo, I. W., Lee, K. K., & Detwiler, R. L. (2015). Tail shortening with developing eddies in a rough-walled rock fracture. *Geophysical Research Letters*, *42*(15), 6340–6347.

Luo, J., Cirpka, O., Wu, W., Fienen, M., Jardine, P., Mehlhorn, T., … Kitanidis, P. (2005). Mass-transfer limitations for nitrate removal in a uranium-contaminated aquifer. *Environmental Science & Technology*, *39*(21), 8453–8459.

Luo, J., Wu, W., Fienen, M., Jardine, P., Mehlhorn, T., Watson, D., … Kitanidis, P. (2006). A nested-cell approach for in situ remediation. *Ground Water*, *44*(2), 266–274.

Moreno, L., Neretnieks, I., & Eriksen, T. (1985). Analysis of some laboratory tracer runs in natural fissures. *Water Resources Research*, *21*(7), 951–958.

Neretnieks, I., Eriksen, T., & Tähtinen, P. (1982). Tracer movement in a single fissure in granitic rock: Some experimental results and their interpretation. *Water Resources Research*, *18*(4), 849–858.

Novakowski, K., Lapcevic, P. A., Voralek, J., & Bickerton, G. (1995). Preliminary interpretation of tracer experiments conducted in a discrete rock fracture under conditions of natural flow. *Geophysical Research Letters*, *22*, 1417–1420.

Qian, J., Chen, Z., Zhan, H., & Luo, S. (2011). Solute transport in a filled single fracture under non-Darcian flow. *International Journal of Rock Mechanics & Mining Sciences*, *48*, 132–140.

Raven, K. G., Novakowski, K. S., & Lapcevic, P. A. (1988). Interpretation of field tracer tests of a single fracture using a transient solute storage model. *Water Resources Research*, *24*(12), 2019–2032.

Richmond, M. C., Perkins, W. A., Scheibe, T. D., Lambert, A., & Wood, B. D. (2013). Flow and axial dispersion in a sinusoidal-walled tube: Effects of inertial and unsteady flows. *Advances in Water Resources*, *62*, 215–226.

Tsang, Y. W., & Tsang, C. F. (1987). Channel model of flow through fractured media. *Water Resources Research*, *23*(3), 467–479.

USEPA. (1996). Pump-and-treat ground-water remediation: A guide for decision makers and practitioners (EPA/625/R-95/005). Office of Research and Development, Washington, D.C.

Voudrias, E. A. (2001). Pump-and-treat remediation of groundwater contaminated by hazardous waste: Can it really be achieved? *Global NEST Journal*, *3*(1), 1–10.

Wang, L., & Cardenas, M. B. (2014). Non-Fickian transport through two-dimensional rough fractures: Assessment and prediction. *Water Resources Research*, *50*, 871–884.

Zheng, C., & Bennett, G. D. (2002). *Applied contaminant transport modeling*. New York, NY: John Wiley & Sons.

Zhou, Q., Liu, H.-H., Bodvarsson, G. S., & Molz, F. J. (2006). Evidence of multi-process matrix diffusion in a single fracture from a field tracer test. *Transport in Porous Media*, *63*, 473–487.

How to cite this article: Lee SH, Yeo IW, Lee K-K, Lee WS. The role of eddies in solute transport and recovery in rock fractures: Implication for groundwater remediation. *Hydrological Processes*. 2017;31:3580–3587. https://doi.org/10.1002/hyp.11283